Low-temperature resistivity from electron–dual-phonon processes for alkali metals

Zhongcheng Wang and G. D. Mahan
Department of Physics and Astronomy, University of Tennessee, Knoxville, Tennesee 37996-1200
(Received 28 October 1988)

A calculation of the contribution from electron–dual-phonon scattering to the low-temperature electrical resistivity for alkali metals is carried out. It is found that the low-temperature resistivity from umklapp electron–dual-phonon scattering processes follows nearly the same exponential rule $BT^4\exp(-\Theta'/T)$ as resulted from umklapp electron–single-phonon scattering, where Θ' is dependent on the minimum available wave vector of phonons and the coefficient B is proportional to $(m/M)^2$, the square of the mass ratio of electron to ion. However, the constant Θ' we find from dual-phonon processes is only half of that from single-phonon processes. It is expected that this scattering mechanism has a significant effect on the low-temperature resistivity of some light alkali metals with high Debye temperature at very low temperatures. Our calculation shows that the resistivity of the lithium that resulted from dual-phonon processes will be larger than the one from single-phonon processes when the temperature is below 4 K.

I. INTRODUCTION

The low-temperature resistivity due to the electron-phonon interaction is usually considered from electron–single-phonon scattering including both normal and umklapp processes. In metals the normal electron–single-phonon scattering provides a T^5 term to the low-temperature resistivity if phonon-drag effects can be neglected. In alkali metals phonon drag is important and eliminates the T^5 term. The umklapp electron–single-phonon scattering provides an exponential decrease term $T^n\exp(-\Theta/T)$, where Θ depends on the minimum wave vector of the involved phonons and n may be 1 to $\frac{7}{2}$ (Ref. 1) (our calculation gives $n=2$). As pointed out in Ref. 2, what value n may be is not important, because the dominant contributions is from the exponential part.

There is another electron-phonon scattering process which also contributes to the resistivity. These are the multiphonon processes suggested by Enz.[2] Multiphonon processes have been included in the calculation of phonon-phonon interaction in the heat transport problem.[3] For electrical transport the calculation has been done for the magneto-optical processes in semiconductors[4] and for the high-temperature resistivity of metals,[5] but not including the low-temperature resistivity. The reasons may be due to (1) the Migdal's theorem,[6] which says that the higher-order electron-phonon interaction only provides a correction of order of magnitude of $(m/M)^n$, where n is the order of interaction; (2) the low-temperature resistivity experiments for simple metals, which can be explained perfectly by the resistivity theory based on the electron–single-phonon process; (3) the contribution from normal electron–dual-phonon processes, which is too small to be invoked to explain the experiments, as we find in the Sec. II; (4) most of contribution from dual-phonon processes will be canceled by single-phonon processes. This is, perhaps, the most important reason, as pointed out by Ngai[4] and Herring,[7] which is discussed now. The electron-ion interaction potential can be expressed as $\sum_n V(\mathbf{r}-\mathbf{R}_n-\mathbf{s}_n)$, where $\mathbf{r}$ is the position vector of electron, $\mathbf{R}_n$ is the position of the nth ion in the equilibrium configuration, and $\mathbf{s}_n$ is the deviation of the nth ion. This potential is expanded as the power series of $\mathbf{s}_n$, and only the second-order term is kept. The electron-phonon Hamiltonian can be written as

$$\begin{aligned} H_{\rm int} &= H^1_{ep}+H^2_{ep}+\cdots , \\ H^1_{ep} &= -\sum_n \mathbf{s}_n\cdot\nabla V(\mathbf{r}-\mathbf{R}_n) , \\ H^2_{ep} &= \tfrac{1}{2}\sum_n \mathbf{s}_n\cdot\nabla\nabla V(\mathbf{r}-\mathbf{R}_n)\cdot\mathbf{s}_n . \end{aligned} \tag{1}$$

The first-order term H^2_{ep} gives rise to electron–single-phonon processes and the second-order term H^2_{ep} gives rise to electron–dual-phonon processes. However, the dual-phonon processes can also arise from the second-order matrix elements of the single-phonon Hamiltonian H^1_{ep}. As described by Herring, most of the acoustic scattering matrix element of H^2_{ep} will be canceled by the second-order matrix elements of H^1_{ep}. This cancellation of terms in the transport formulation has made it difficult to draw any conclusions from transport data concerning the importance of the bilinear acoustic term, H^2_{ep}. Therefore, it seems that the higher-order electron-phonon correction is not necessary. However, our calculation for electron–dual-phonon interaction shows that (a) the reason (4) mentioned above does not apply to umklapp electron–dual-phonon processes; (b) at very low temperatures the higher-order electron-phonon interaction is important. The physical origin is that the contribution to the resistivity from normal electron-phonon interaction is canceled due to the phonon-drag effects and only umklapp processes contribute to the resistivity. The resistivity follows the general exponential decrease relation

$BT^n \exp(-\Theta/T)$. The critical parameter Θ depends on the minimum wave vector of the phonons involved in umklapp processes. The dual-phonon processes will reduce the constant Θ by half. Therefore, at very low temperatures, the reduction of coefficient by m/M may be offset by the increase of the exponential part.

In this paper we consider electron–dual-phonon processes in alkali metals. Two limit cases are considered: (1) the Bloch limit, in which the phonon system in equilibrium state is assumed and only the normal scattering processes are considered; (2) the phonon-drag limit, in which only umklapp scattering processes are considered. The Matsubara Green's-function method is used to calculate the self-energy from electron–dual-phonon scattering processes. It is found that in the Bloch limit, the contribution from the dual-phonon processes provides a T^7 term to the low-temperature resistivity for alkali metals. The coefficient of this term is proportional to the $(m/M)^2$. In comparison with the Bloch T^5 term, this term can be neglected. In the phonon-drag limit, it is found that umklapp dual-phonon processes provide a $BT^4 \exp(-\Theta'/T)$ as umklapp single-phonon processes do. In the single-phonon scattering processes the minimum wave vector and the phonons equals $G-2k_F$, where G and k_F are the vector of the reciprocal lattice and the Fermi wave vector, respectively, and Θ can be approximately expressed as $0.2\Theta_D$.[8] However, the minimum available wave vector in dual-phonon processes is only half of the one in single-phonon processes.

The contributions from the second-order matrix elements of the single-phonon Hamiltonian H^1_{ep} for umklapp scattering are examined in Appendix A. It is found that all these contributions are proportional to $(m/M)^2$ and $\exp(-\Theta/T)$. But they have nothing to do with $BT^4 \exp(-\Theta'/T)$ term.

The magnitude of this term for alkali metals with small ion mass and large Θ_D, for example, Li, is expected to be compared with the one due to single-phonon processes at some very low temperatures. In order to compare directly, the calculation of the resistivity resulted from umklapp single-phonon processes, using Matsubara Green's-function method, is given in the Appendix B. It is found that the resistivity for lithium from dual-phonon processes will be larger than the one from single-phonon processes when the temperature is below 4 K.

The electron–dual-phonon Hamiltonians are derived as follows. The derivation $\mathbf{s}_n$ is expressed as the normal coordinates

$$\mathbf{s}_n=\sum_{\mathbf{q},\lambda}\left[\frac{1}{2nM\omega_{\mathbf{q}\lambda}}\right]^{1/2}\exp(i\mathbf{q}\cdot\mathbf{R}_n)(a_{\mathbf{q}\lambda}+a^{\dagger}_{-\mathbf{q},\lambda}) . \tag{2}$$

Then the electron-phonon interaction Hamiltonian describing dual-phonon processes is written as follows:

$$H_{\rm int}=-\tfrac{1}{2}\sum_{\mathbf{q}_1,\mathbf{q}_2}\sum_{\mathbf{k},\mathbf{G}}\sum_{\lambda_1,\lambda_2}M_{\mathbf{q}_1\lambda_1,\mathbf{q}_2\lambda_2,\mathbf{G}}C^{\dagger}_{\mathbf{k}+\mathbf{q}_1+\mathbf{q}_2+\mathbf{G}} \times C_{\mathbf{k}}(a_{\mathbf{q}_1\lambda_1}+a^{\dagger}_{-\mathbf{q}_1\lambda_1}) \times(a_{\mathbf{q}_2\lambda_2}+a^{\dagger}_{-\mathbf{q}_2\lambda_2}) , \tag{3}$$

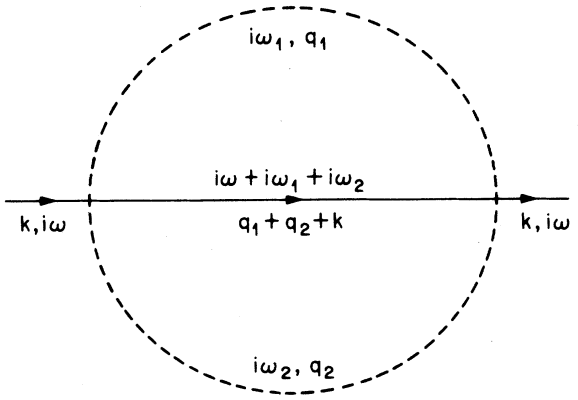

FIG. 1. The Feynman diagram of the electron–dual-phonon interaction.

$$M_{\mathbf{q}_1\lambda_1,\mathbf{q}_2\lambda_1\mathbf{G}}=\left[\frac{1}{4(nM)^2\omega_{\mathbf{q}_1\lambda_1}\omega_{\mathbf{q}_2\lambda_2}}\right]^{1/2} \times V(|\mathbf{q}_1+\mathbf{q}_2+\mathbf{G}|)[(\mathbf{q}_1+\mathbf{q}_2+\mathbf{G})\cdot\hat{\mathbf{e}}_{\mathbf{q}_1\lambda}] \times[(\mathbf{q}_1+\mathbf{q}_2+\mathbf{G})\cdot\hat{\mathbf{e}}_{\mathbf{q}_2\lambda}] ,$$

where nM is the mass density of the ion. The Feynman diagram used in the calculation is shown in Fig. 1.

The electron and phonon Matsubara Green's functions are defined, respectively, as follows:

$$\mathbf{G}^0(\mathbf{k},i\omega)=\frac{1}{i\omega-\xi_{\mathbf{k}}} , \tag{4}$$

$$D^0_{\lambda}(\mathbf{q},i\omega)=-\frac{2\omega_{\lambda,\mathbf{q}}}{\omega^2+\omega^2_{\lambda,\mathbf{q}}} , \tag{5}$$

where $\xi_{\mathbf{k}}=\epsilon_{\mathbf{k}}-\mu$.

The self-energy of electron using Matsubara Green's function method[9] is expressed as

$$\Sigma(\mathbf{p},i\omega)=(1/\beta^2)\sum_{i\omega_1\lambda_1}\sum_{i\omega_2\lambda_2}\sum_{\mathbf{G}}\int\frac{d^3q_1}{(2\pi)^3} \times\int\frac{d^3q_2}{(2\pi)^3}M^2_{\mathbf{q}_1\lambda_1,\mathbf{q}_2\lambda_2,\mathbf{G}} , \tag{6}$$
$$\mathbf{G}^0(\mathbf{p}+\mathbf{q}_1+\mathbf{q}_2+\mathbf{G}, i\omega+i\omega_1+i\omega_2)D^0_{\lambda_1}(\mathbf{q}_1,i\omega_1)D^0_{\lambda_2}(\mathbf{q}_2,i\omega_2) .$$

The further calculation of Eq. (6) will be done in two limit cases: (1) normal scattering processes; (2) umklapp scattering processes.

II. NORMAL ELECTRON–DUAL-PHONON SCATTERING PROCESSES

The Bloch limit is considered first. Let $\mathbf{G}$ be zero. The electron-ion potential in Eq. (3) is written in the form of the model pseudopotential[10]

$$V(q)=\frac{-2/3E_F+(q/q_{\rm TF})^2 w(q)}{1+(q/q_{\rm TF})^2}\ ,$$
$$q_{\rm TF}^2=\frac{6\pi e^2 n}{E_F}\ , \tag{7}$$

where $w(q)$ is the model pseudopotential of simple metals and $q_{\rm TF}$ is the Thomas-Fermi screening wave vector. At low temperatures, the dominant contribution for normal electron-phonon processes is from the phonons whose wave vectors q are much smaller than $q_{\rm TF}$ and it is a good approximation to rewrite $V(q)\approx V(0)=-\frac{2}{3}E_F$. In order to make the problem tractable, we use the same dispersion relation, $\omega_q\approx\bar{c}q$ for both polarizations and $\bar{c}$ is the average velocity of phonons. Therefore the polarization subscription of ω_q can be suppressed. Do summations over ω_1 and ω_2 and then do analytic continuation from $i\omega$ to $\omega+i\delta$. The imaginary part of the self-energy from Eq. (6) is derived as follows:

$$\begin{aligned}
&{\rm Im}\Sigma(\mathbf{p},\omega)\\
&=-\pi\sum_{\lambda_2,\lambda_1}\int\frac{d^3q_1}{(2\pi)^3}\frac{d^3q_2}{(2\pi)^3}M^2_{\mathbf{q}_1\lambda_1,\mathbf{q}_2\lambda_2}\\
&\quad\times[\Psi_1\delta(1)+\Psi_2\delta(2)+\Psi_3\delta(3)+\Psi_4\delta(4)]\ ,\\
&\Psi_1=[n_B(\omega_{\mathbf{q}_2})+n_F(\omega_{\mathbf{q}_2}-\omega)]\\
&\quad\times[n_B(\omega_{\mathbf{q}_1})+n_F(\omega_{\mathbf{q}_1}+\omega_{\mathbf{q}_2}-\omega)]\ ,\\
&\Psi_2=[n_B(\omega_{\mathbf{q}_2})+n_F(\omega_{\mathbf{q}_2}+\omega)]\\
&\quad\times[n_B(\omega_{\mathbf{q}_1})+n_F(\omega_{\mathbf{q}_1}-\omega_{\mathbf{q}_2}-\omega)]\ ,\\
&\Psi_3=[n_B(\omega_{\mathbf{q}_2})+n_F(\omega_{\mathbf{q}_2}-\omega)][n_B(\omega_{\mathbf{q}_1}-\omega_{\mathbf{q}_2}+\omega)]\ ,\\
&\Psi_4=[n_B(\omega_{\mathbf{q}_2})+n_F(\omega_{\mathbf{q}_2}+\omega)]\\
&\quad\times[n_B(\omega_{\mathbf{q}_1})+n_F(\omega_{\mathbf{q}_1}+\omega_{\mathbf{q}_2}+\omega)]\ ,\\
&\delta(1)=\delta(\omega-\omega_{\mathbf{q}_1}-\omega_{\mathbf{q}_2}-\xi_{\mathbf{p}+\mathbf{q}_1+\mathbf{q}_2})\ ,\\
&\delta(2)=\delta(\omega-\omega_{\mathbf{q}_1}+\omega_{\mathbf{q}_2}-\xi_{\mathbf{p}+\mathbf{q}_1+\mathbf{q}_2})\ ,\\
&\delta(3)=\delta(\omega+\omega_{\mathbf{q}_1}-\omega_{\mathbf{q}_2}-\xi_{\mathbf{p}+\mathbf{q}_1+\mathbf{q}_2})\ ,\\
&\delta(4)=\delta(\omega+\omega_{\mathbf{q}_1}+\omega_{\mathbf{q}_2}-\xi_{\mathbf{p}+\mathbf{q}_1+\mathbf{q}_2})\ ,
\end{aligned} \tag{8}$$

where $n_B(x)$ and $n_F(x)$ are the Bose and Fermi distribution functions, respectively. They are defined as follows:

$$n_B(x)=\frac{1}{e^{\beta x}-1},\quad n_F(x)=\frac{1}{e^{\beta x}+1}$$

with $\beta=1/T$. Let $\mathbf{q}_1+\mathbf{q}_2=\mathbf{Q}$. We introduce the following function:

$$H(u_1,u_2)=-\pi\sum_{\lambda_1,\lambda_2}\int\frac{d^3q_1}{(2\pi)^3}\frac{d^3q_2}{(2\pi)^3}M^2_{\mathbf{q}_1\lambda_1,\mathbf{q}_2\lambda_2}\delta(\mathbf{p}\cdot\mathbf{Q}/m+Q^2/2m\pm\omega_{\mathbf{q}_1}\pm\omega_{\mathbf{q}_2})\delta(u_1-\omega_{\mathbf{q}_1})\delta(u_2-\omega_{\mathbf{q}_2})\ . \tag{9}$$

In dual-phonon processes the phonons of both longitudinal and transverse polarization can scatter electrons. We choose one transverse polarization in the q_1-q_2 plane and another one perpendicular to this plane. Only the phonons of former transverse polarization contribute to scattering. There are four possible combinations of polarizations from two phonons. α_1 is denoted as the angle between $\mathbf{Q}$ and $\mathbf{q}_1$, α_2 is denoted as the angle between $\mathbf{Q}$ and $\mathbf{q}_2$, $\bar{\theta}$ is denoted as the angle between $\mathbf{q}_1$ and $\mathbf{q}_2$, and $\bar{\beta}$ is denoted as the angle between $\mathbf{Q}$ and $\mathbf{k}$ as shown in Fig. 2. The polarization factor is $Q^4\cos^2\alpha_1\cos^2\alpha_2$ if both phonons are longitudinal, $Q^4\cos^2\alpha_1\sin^2\alpha_2$ if one phonon is longitudinal and the other is transverse and $Q^4\sin^2\alpha_1\sin^2\alpha_2$ if both phonons are transverse. The summation over polarization modes gives factor Q^4. The H function is evaluated by changing the integral variable as follows:

$$\int\frac{d^2q_1}{(2\pi)^3}\frac{d^3q_2}{(2\pi)^3}\rightarrow\frac{1}{(2\pi)^4 v_F}\int q_1dq_1\int q_2dq_2\int dQ\int d(Qk\cos\bar{\beta})\ . \tag{10}$$

The conditions of the momentum conservation in the four δ functions of Eq. (9) are the same, because $(\mathbf{k}+\mathbf{Q})^2/2m\approx k^2/2m\approx\mu$ and $\omega_{\mathbf{q}_1},\omega_{\mathbf{q}_2}\ll\mu$. The integral limit of Q is from $|q_1-q_2|$ to (q_1+q_2). For convenience, $H^>$ is denoted for the $q_1>q_2$ case and $H^<$ is for the $q_1<q_2$ case. It is easy to see that $H^>(u_1,u_2)=H^<(u_2,u_1)$. Because only the even part of ${\rm Im}\Sigma(\omega)$ contributes the conductivity of metals, the δ function can be expanded at $\omega=0$, and only the first term is kept. The δ function can be integrated first. Then we obtain

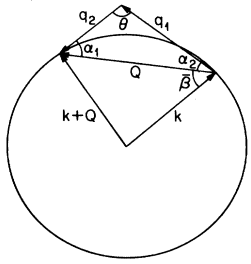

FIG. 2. The normal electron–dual-phonon scattering processes in momentum space.

$$H^{>}(u_1,u_2)=-\frac{\pi|V(0)|^2}{(4\pi)^4(nM)^2v_Fc^{-9}}J(u_1,u_2)\ , \tag{11}$$

$$J(u_1,u_2)=2u_1^4u_2+4u_1^2u_2^3+0.4u_2^5\ . \tag{12}$$

For the same reason, $\Psi_1+\Psi_2+\Psi_3+\Psi_4$ can also be expanded as the power series of ω and only the first term is kept:

$$\Psi_1+\Psi_2+\Psi_3+\Psi_4=2[n_B(u_2)+n_F(u_2)]\times[2n_B(u_1)+n_F(u_1+u_2)+n_F(u_1-u_2)]+O(\omega^2)\ . \tag{13}$$

Make variable change $x_1=\beta u_1$ and $x_2=\beta u_2$, then the $\mathrm{Im}\Sigma(\mathbf{p},\omega)$ is

$$\mathrm{Im}\Sigma(\mathbf{p},\omega)=2T^7\int_0^\infty dx_2[n_B(x_2)+n_F(x_2)]\left[\int_0^{x_2}dx_1H^{<}(x_1,x_2)[2n_B(x_1)+n_F(x_1-x_2)+n_F(x_1+x_2)]+\int_{x_2}^\infty dx_1H^{>}(x_1,x_2)[2n_B(x_1)+n_F(x_1-x_2)+n_F(x_1+x_2)]\right]\ ,$$

where the up integral limit can extend to ∞ at low temperatures. From $1/\tau=-2\,\mathrm{Im}\Sigma$, the resistivity is calculated from

$$\sigma=\frac{m}{ne^2\tau}\ ,$$

$$\tau^{-1}=\frac{\pi}{4^6}E_F\left[\frac{m}{M}\right]^2\left[\frac{v_F}{c}\right]^9\left[\frac{T}{E_F}\right]^7I\ , \tag{14}$$

$$I=\int_0^\infty dx_2[n_B(x_2)+n_F(x_2)]\left[\int_0^{x_2}dx_1J(x_1,x_2)[2n_B(x_1)+n_F(x_1-x_2)+n_F(x_1+x_2)]+\int_{x_2}^\infty dx_1J(x_2,x_1)[2n_B(x_1)+n_F(x_1-x_2)+n_F(x_1+x_2)]\right]\ .$$

It gives T^7 contribution to the low-temperature resistivity. The coefficient of this term is proportional to $(m/M)^2$. At low temperatures this scattering mechanism is much smaller than the Bloch T^5 term. Perhaps this term cannot be observed experimentally at any temperatures. So, it is not necessary to examine the cancellation of this term by the second-order matrix elements from the single-phonon Hamiltonian H_{ep}^1.

III. UMKLAPP SCATTERING PROCESSES

Umklapp electron–dual-phonon scattering processes are different from normal scatting processes in the following ways.

(1) The addition of the wave vectors of the two phonons involved in umklapp electron–dual-phonon scattering will be fixed by the condition $\mathbf{Q}=\mathbf{k}'-\mathbf{k}-\mathbf{G}$. The momentum conservation condition restricts the phonons by wave vectors in low limits. The definition of the H function should be modified by adding any arbitrary vector of the reciprocal lattice.

(2) The wave vectors of phonons involved in umklapp processes are much larger than in normal processes. The dispersion relation should change. However, the Bose distribution has an exponential decrease for high-energy phonons. The phonons involved in umklapp processes are also restricted by the wave vector. Therefore, the same formula $\omega_q=\bar{c}q$ can be approximately used to describe the phonons for umklapp processes but with different propaganda velocity $\bar{c}$.[1] For simplicity, we still use approximately the same dispersion relation for two kinds of polarizations.

(3) The electron-ion interaction potential changes. From Eq. (7), the potential $V(q)$ is very sensitive to argument q when q is large to be compared with $2k_F$. In order to obtain the quantitative result, the electron-ion po-

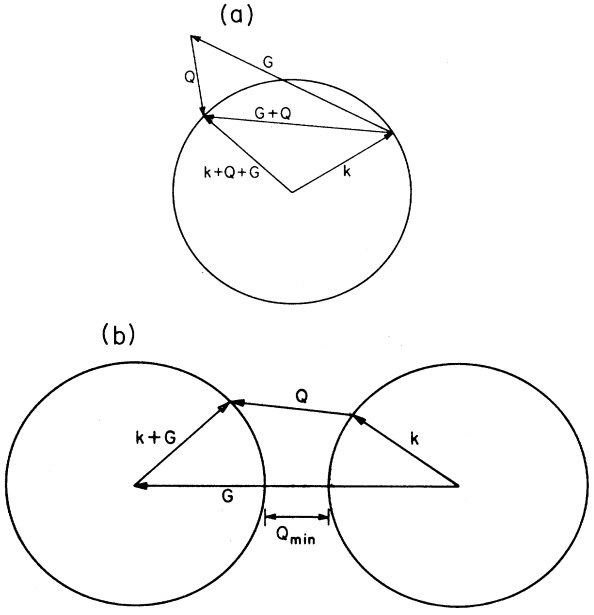

FIG. 3. The umklapp electron–dual-phonon scattering processes in ordinary momentum space (a) and in the repeat zone scheme (b).

tential is written in the simplified form:[12]

$$V(q)=-\frac{2k_F}{3}\frac{\cos(qr_c)}{1+(q/q_{\rm TF})^2}. \tag{15}$$

(4) The change of the momentum between two electron states involved in umklapp processes is $\mathbf{Q}+\mathbf{G}$. The polarization factor for umklapp processes in this case gives $(\mathbf{Q}+\mathbf{G})^4$. This is derived from the following consideration. Consider the polarization factor of phonon $\mathbf{q}_1$ in Fig. 3(a). One of the transverse polarizations of phonon $\mathbf{q}_1$ is chosen in the plane defined by $\mathbf{q}_1$ and $\mathbf{G}+\mathbf{Q}$, another one is chosen perpendicular to this plane, and α_1 is denoted as the angle between $\mathbf{q}_1$ and $\mathbf{Q}+\mathbf{G}$. Then, the square of the longitudinal polarization factor from phonon $\mathbf{q}_1$ is $\cos^2\alpha_1(\mathbf{G}+\mathbf{Q})^2$. The square of the transverse polarization factor is $\sin^2\alpha_1(\mathbf{G}+\mathbf{Q})^2$. From approximation (3), the total polarization factor from the phonon $\mathbf{q}_1$ is $(\mathbf{Q}+\mathbf{G})^2$. In the same way phonon $\mathbf{q}_2$ gives the same polarization factor.

(5) The vectors of the reciprocal lattice are located at the special directions at the momentum space. It will give different possibility of electrons with the different initial state of electrons. It must average momentum state of electrons over the Fermi surface. $\tilde{\beta}$ is denoted as the angle between $\mathbf{p}$ and $\mathbf{Q}+\mathbf{G}$. Then this average is expressed as $\int d\cos\tilde{\beta}/2$. Remembering all these differences between normal and umklapp processes, we introduce the following new $\bar{H}$ function for umklapp processes:

$$\tilde{H}(u_1,u_2)=-\frac{\pi z}{8(nM)^2\tilde{c}^2}\int\frac{d^3q_1}{(2\pi)^3}\frac{d^3q_2}{(2\pi)^3}\frac{d\cos\tilde{\beta}}{q_1q_2}(\mathbf{G}+\mathbf{Q})^4V(|\mathbf{G}+\mathbf{Q}|)^2\delta(\xi_{\mathbf{p}+\mathbf{Q}+\mathbf{G}}-\xi_{\mathbf{q}}\pm\omega_{q_1}\pm\omega_{q_2})\delta(v_1-\omega_{q_1})\delta(u_2-\omega_{q_2}), \tag{16}$$

where z is the number of the nearest vectors of the reciprocal lattice. The integrals of the colatitude angles α_i and $\tilde{\theta}$ of the two phonons are changed, respectively, as follows:

$$\int q_1q_2d\cos\tilde{\theta}\to\int_{Q_{\min}\text{ or }|u_1-u_2|/2k_F\tilde{c}}^{2\omega_D}Q\,dQ\int d\cos\alpha_i \to\int_{G-Q}^{2k_F}\frac{|\mathbf{G}+\mathbf{Q}|d|\mathbf{G}+\mathbf{Q}|}{GQ}.$$

Unlike the normal dual-phonon scattering case, the momentum conservation for umklapp processes requiring that $q_1+q_2\geq Q\geq\max\{Q_{\min},|q_1-q_2|\}$, the low-integral limit of dQ is the bigger one of $|q_1-q_2|$ and $Q_{\min}$. As shown in Figs. 3(a) and 3(b), the minimum wave vector of $Q_{\min}$ involved in umklapp processes is $G-2k_F$. It will be clear later on that the dominant contribution is from the two phonons with nearly the same wave vectors. Therefore, the low-integral limit can be chosen to be just $Q_{\min}$. This simplifies $\bar{H}(u_1,u_2)$ greatly. It allows $\bar{H}(u_1,u_2)$ to only depend on u_1+u_2 not on the two-independent variables u_1 and u_2. We denote the corresponding minimum energy of phonons involved by $\Theta=\tilde{c}Q_{\min}$. After finishing the integral of the δ function, the $\bar{H}$ function becomes

$$\bar{H}(u_1,u_2)=-C\int_{\Theta/2k_F\tilde{c}}^{(u_1+u_2)/2k_F\tilde{c}}dx\,J(x-\Theta/2k_F\tilde{c}), \tag{17}$$

$$J(x)=\int_{1-x}^{1}dy'\left[\frac{y'^2\cos(\alpha_0y')}{1+\gamma y'^2}\right]^2,$$

$$C=\frac{\pi z(2k_F)^6}{(4\pi)^4G(nM)^2v_F\tilde{c}^4}\left[\frac{2E_F}{3}\right]^2, \tag{18}$$

$$\alpha_0=2r_ck_F,$$

$$\gamma=(2k_F/q_{\rm TF})^2.$$

For convenience, we have introduced the $J(x)$ function with $x=(Q-Q_{\min})/2k_F$. The self-energy of the electron from umklapp electron–dual-phonon scattering processes is

$$\mathrm{Im}\Sigma(\mathbf{p},\omega)=2\int du_1du_2\bar{H}(u_1+u_2)[n_B(u_2)+n_F(u_2)]\times[2n_B(u_1)+n_F(u_1-u_2)+n_F(u_1+u_2)], \tag{19}$$

where the integral limits is determined by the condition that $\Theta\leq\{u_1+u_2\}\leq2\Theta_D$. The evaluation of Eq. (19) begins with the integral of u_1 by parts. It is worth noting that the $\bar{H}(u)$ in Eq. (17), in fact, is dependent on $u/2k_F\tilde{c}$, so at very low temperatures, the three terms in the second square bracket of Eq. (19) become δ-like functions. It is easy to see that the dominant contribution is from the middle term. Because of the condition $u_1+u_2\geq\Theta$, the peaks of the other two terms in the square bracket of Eq. (19) are out of range and only the middle term $-\partial n_F(u_1-u_2)/\partial u_1=\delta(u_1-u_2)$ has a peak when $u_1=u_2$. Equation (19) now becomes

$$\mathrm{Im}\Sigma(\mathbf{p},\omega)=2\int_{\Theta/2}^{\omega_D}du[n_B(u)+n_F(u)]\int_{\Theta}^{2u}dy\,\bar{H}(y). \tag{20}$$

Because of the sharp decrease of $n_F(u)$ and $n_B(u)$ for large u, the main contribution in integral of $\bar{H}(y)$ in Eq. (17) is from $y\approx\Theta/2k_F\tilde{c}$. Then we have

$$J(x)\approx\left[\frac{\cos\alpha_0}{(1+\gamma)}\right]^2x+O(x^2),$$

$$\bar{H}(y)\approx-\frac{C}{2}\left[\frac{\cos\alpha_0}{(1+\gamma)}\right]^2\left[y-\frac{\Theta}{2k_F\tilde{c}}\right]^2 =-\frac{\pi z(2k_F)^6V(2k_F)^2}{2(4\pi)^4G(nM)^2v_F\tilde{c}^4}\left[y-\frac{\Theta}{2k_F\tilde{c}}\right]^2.$$

It is a good approximation to replace the Bose and Fermi distribution $n_B(u_2)$ and $n_F(u_2)$ each by the Maxwell dis-

tribution $\exp(-u_2/T)$. Then the integral of u can be done easily. The low-temperature resistivity from dual-phonon processes is derived as follows:

$$\rho_{\rm dph}=\frac{m}{ne^2\tau}=BT^4\exp(-\Theta/2T)\ , \tag{21}$$

$$B_{\rm dph}=\frac{z}{4\pi^3}\frac{m}{ne^2}\frac{(2k_F)^4}{(nM)^2v_F\bar{c}^{\,6}G}[gV(g)]^2_{g=2k_F}\ .$$

The numerical calculation is done for lithium. Some

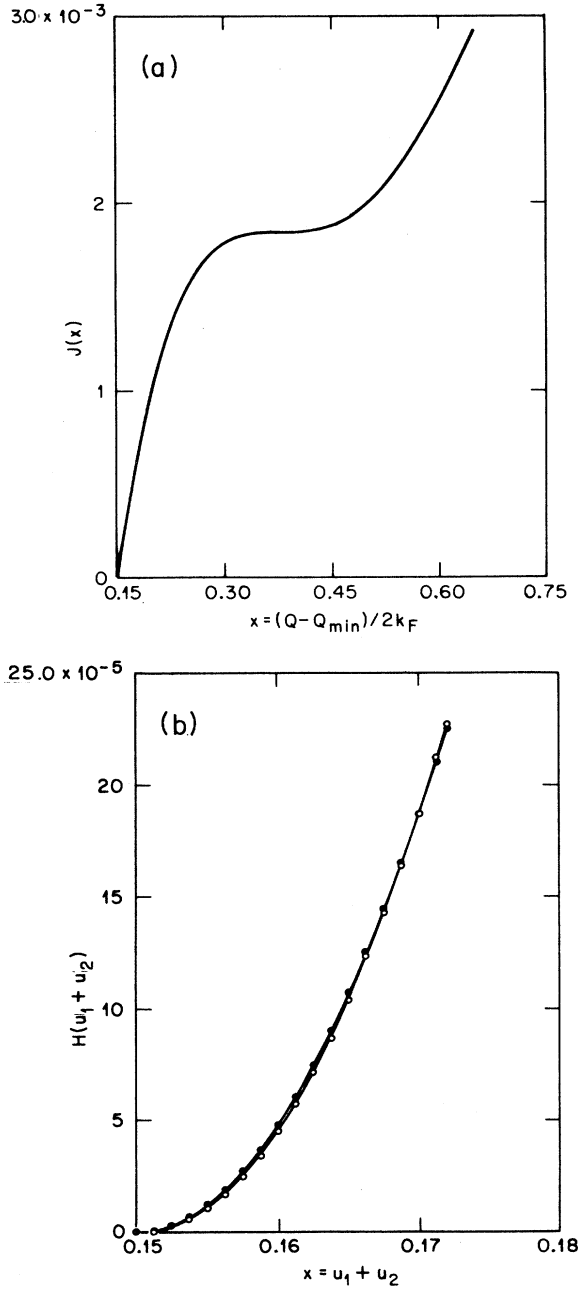

FIG. 4. (a) The plot of $J(x-\Theta/2k_F\bar{c})$, where $x=Q/2k_F$. (b) The plot of $H(u_1+u_2)$ and its fitting line $y(x)=0.48(x-\Theta)^2$. The line with the solid circle is for $H(u_1+u_2)$ and the asterisk for $y(x)$.

TABLE I. The crystal parameters of lithium (Refs. 11 and 12). n is the density of electron and a is for crystal constant.

n	$=4.7\times10^{22}$ cm^{-3}
k_F	$=1.11\times10^{8}$ cm^{-1}
v_F	$=4.7\times10^{22}$ cm/sec
z	$=12$
a	$=3.491\times10^{-8}$ cm
G	$=2.55\times10^{8}$ cm^{-1}
r_c	$=0.92\times10^{-8}$ cm
$q_{\rm TF}$	$=1.64\times10^{8}$ cm^{-1}
Θ_D	$=330$ K

useful crystal parameters are listed in Table I. In order to obtain quantitative result, the crystal structure of lithium, at very low temperatures, is still assumed as bcc, though recent neutron scattering experiments reveal that it is a $9R$ structure below transition temperature of 70 K.[13]

The plots of $J(x-\Theta/2k_F\bar{c})$ and $\bar{H}(y)$ are given in Figs. 4(a) and 4(b). $\bar{H}(y)$ can be replaced by $0.45C(y-\Theta/2k_F\bar{c})^2$ as shown in Fig. 4(b).

In the coefficient B, only $\bar{c}$ is difficult to be determined. The average sound velocity in lithium crystal is nearly 5×10^5. However, the $\bar{c}$ should be much smaller than the average sound velocity c, since (1) $\bar{c}$ is the average velocity measured at $q=Q_{\rm min}/2=(G-2k_F)/2$, and c is at $q=0$; (2) $\bar{c}^{\,-6}$ favors smallest values of $\bar{c}$. According to the empirical relation $Q_{\rm min}\bar{c}=0.2\Theta_D$, $\bar{c}\approx2.6\times10^5$ can be obtained. Considering above reason (2), we take $\bar{c}\approx2\times10^5$, then $B_{\rm dph}=1.0\times10^{-15}\ \Omega\,{\rm mK}^{-4}$. Since the theoretical result of the resistivity for umklapp single-phonon processes is only available from the variational calculation, in order to compare our result with the one from single-phonon processes directly, the calculation of resistivity for single-phonon based on the Matsubara method is given in Appendix B. The ratio of resistivity of dual phonon to single phonon can be derived from Eq. (24) as

$$\frac{\rho_{\rm dph}}{\rho_{\rm sph}}=\frac{B_{\rm dph}}{B_{\rm sph}}\approx\frac{T^2E_F}{(k_F\bar{c})^3}\frac{m}{M}e^{\Theta/2T}\ . \tag{22}$$

It is found that the resistivity resulted from dual-phonon process will be larger than the one due to the single-phonon process below 4K.

IV. CONCLUSION

In this paper, we calculate the contribution from electron–dual-phonon scattering including both normal and umklapp processes to the low-temperature electrical resistivity for alkali metals. It is found that the contribution from normal electron–dual-phonon scattering provides the low-temperature resistivity a T^7 term, and its coefficient is proportional to $(m/M)^2$. It follows that the magnitude of this term is smaller than the Bloch T^5 term. It is hard to be observed in the temperature resistivity experiments. Considering umklapp processes it is found that the low-temperature resistivity caused by electron–dual-phonon scattering follows nearly

the same exponential decrease temperature relation $B_{\rm dph}T^4\exp(-\Theta'/T)$ as by electron–single-phonon scattering but with the different parameters. The coefficient $B_{\rm dph}$ is proportional to $(m/M)^2$, and Θ' is only half of Θ. This reduction for the exponential function is significant for low-temperature resistivity of alkali metals, especially for metals with high Θ_D. According to our calculation, the resistivity from dual-phonon processes will be larger than the one from single-phonon processes when the temperature is below $T\approx 4$ K. However, this term is difficult to be detected in the lithium resistivity experiments. This is because the T^2 terms due to electron-electron interaction and inelastic impurity scattering begin appearing at $T\approx 10$ K. These two terms will be dominant below this temperature.[14] In Appendix B, we also consider the contributions from the second-order interaction from the single-phonon Hamiltonian H_{ep}^1. It is found that these contributions do not affect our results.

ACKNOWLEDGMENTS

This work is supported by the National Science Foundation through Grant No. DMR-8704210.

APPENDIX A

There are only two self-energy diagrams for the second-order interaction from the single-phonon Hamiltonian H_{ep}^1 which are related to our problem. These two diagrams are shown in Figs. 5(a) and 5(b), which may cancel the $BT^4\exp(-\Theta'/T)$ term. They can be written as follows:

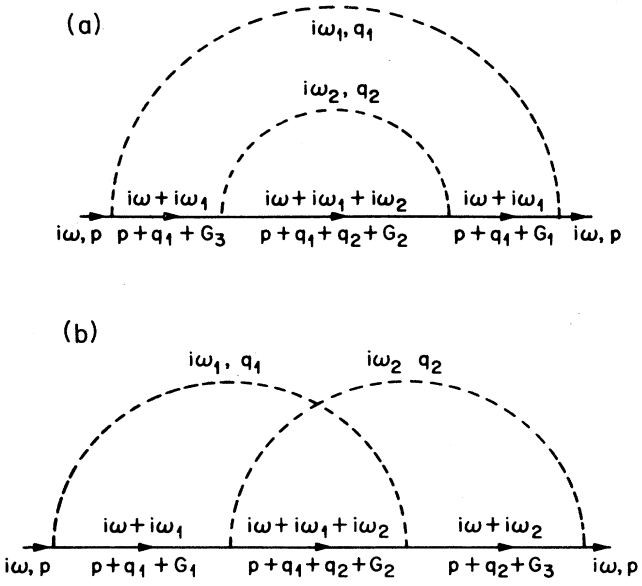

FIG. 5. The Feynman diagrams for the contributions from the second-order matrix elements of single-phonon Hamiltonian H_{ep}^1. There are three diagrams which are shown (a) and (b), respectively.

$$\Sigma^a(\mathbf{p},\omega)=\left[\frac{1}{\beta^2}\right]\sum_{\omega_1,\omega_2}\sum_{\mathbf{q}_1,\mathbf{q}_2}\sum_{\mathbf{G}_1,\mathbf{G}_2}\sum_{\mathbf{G}_3}M_{\mathbf{q}_1}^2M_{\mathbf{q}_2}^2\frac{2\omega_{\mathbf{q}_1}}{\omega_1^2+\omega_{\mathbf{q}_1}^2}\frac{2\omega_{\mathbf{q}_2}}{\omega_2^2+\omega_{\mathbf{q}_2}^2}\frac{1}{i\omega+i\omega_1-\xi_{\mathbf{p}+\mathbf{q}_1+\mathbf{G}_1}}\frac{1}{i\omega+i\omega_1-\xi_{\mathbf{p}+\mathbf{q}_1+\mathbf{G}_3}}$$
$$\times\frac{1}{i\omega+i\omega_1+i\omega_2-\xi_{\mathbf{p}+\mathbf{q}_1+\mathbf{q}_2+\mathbf{G}_2}},$$

$$\Sigma^b(\mathbf{p},\omega)=\left[\frac{1}{\beta^2}\right]\sum_{\omega_1,\omega_2}\sum_{\mathbf{q}_1,\mathbf{q}_2}\sum_{\mathbf{G}_1,\mathbf{G}_2}\sum_{\mathbf{G}_3}M_{\mathbf{q}_1}^2M_{\mathbf{q}_2}^2\frac{2\omega_{\mathbf{q}_1}}{\omega_1^2+\omega_{\mathbf{q}_1}^2}\frac{2\omega_{\mathbf{q}_2}}{\omega_2^2+\omega_{\mathbf{q}_2}^2}\frac{1}{i\omega+i\omega_1-\xi_{\mathbf{p}+\mathbf{q}_1+\mathbf{G}_1}}\frac{1}{i\omega+i\omega_2-\xi_{\mathbf{p}+\mathbf{q}_2+\mathbf{G}_3}}$$
$$\times\frac{1}{i\omega+\omega_1+\omega_2-\xi_{\mathbf{p}+\mathbf{q}_1+\mathbf{q}_2+\mathbf{G}_2}}.$$

These two diagrams have similar structure. In each of these two diagrams, there are three intermediate states available for scattered electron. In diagram (a), electron is scattered from the initial momentum state $\mathbf{p}$ through three intermediate states and finally back to the initial state $\mathbf{p}$ as follows: $\mathbf{p}\rightarrow\mathbf{p}+\mathbf{q}_1+\mathbf{G}_1\rightarrow\mathbf{p}+\mathbf{q}_1+\mathbf{q}_2+\mathbf{G}_2\rightarrow\mathbf{p}+\mathbf{q}+\mathbf{G}_3\rightarrow\mathbf{p}$. Only the last intermediate state in these two diagrams is different.

From the calculation of Eq. (19), the essential condition for obtaining $BT^4\exp(-\Theta'/T)$ term is that the low limits of the momentum integrals q_1 and q_2 must satisfy $q_1+q_2\geq q_{\rm min}$ for intermediate states.

In these two diagrams, if the first intermediate state is an umklapp process, then the low limit of the momentum integral q_1 will be from $q_{\rm min}$ and the above essential condition is not satisfied; if the first intermediate state is normal process, the above essential condition is not satisfied either. Therefore, the two diagrams cannot give rise to the $T^4\exp(-\Theta'/T)$ term.

We conclude our discussion by noting that the $BT^4\exp(-\Theta'/T)$ term due to dual-phonon processes cannot be canceled by the second-order matrix element of the single-phonon Hamiltonian H_{ep}^1.

APPENDIX B

The self-energy for umklapp single-phonon processes can be derived using Matsubara Green's-function method

as follows:

$$\Sigma(\mathbf{p},i\omega_n)=-1/\beta\sum_{iq_n}\sum_{\mathbf{G}}\sum_{\lambda}\int\frac{d^3q}{(2\pi)^3}M^2_{\mathbf{q}+\mathbf{G},\lambda}\times G^0(\mathbf{p}+\mathbf{q}+\mathbf{G},i\omega_n+iq_n)\times D^0_{\lambda}(\mathbf{q},iq_n)\ , \tag{B1}$$

$$M_{\mathbf{q}+\mathbf{G}}=\left[\frac{1}{2nM\omega_{q,\lambda}}\right]^{1/2}V(\mathbf{q}+\mathbf{G})(\mathbf{q}+\mathbf{G})\cdot\hat{\mathbf{e}}_{\mathbf{q}\lambda}\ .$$

This expression has many similarities as the one for dual-phonon processes as follows: (1) the phonons of both longitudinal and transverse polarization can scatter electrons. As in the dual-phonon case, the summation over polarization modes gives a polarization factor $|\mathbf{G}+\mathbf{q}|^2$; (2) the electron-ion interaction potential can be approximately written as $V(2k_F)$; (3) the δ function for energy and the momentum conservation condition has the same form except that $\mathbf{Q}$ is replaced by $\mathbf{q}$.

The resistivity formula for the umklapp single-phonon process is

$$\rho_{\rm sph}=\frac{m}{ne^2\tau}\ ,$$
$$\tau=B_{\rm sph}T^2e^{-\Theta/T}\ , \tag{B2}$$
$$B_{\rm sph}=\frac{z}{4\pi}\frac{1}{nM\tilde{c}^3Gv_F}[GV(g)]^2_{g=2k_F}\times\left[1-\frac{T}{k_F\tilde{c}}+\frac{1}{2}\left[\frac{T}{k_F\tilde{c}}\right]^2\right]\ .$$

At low temperatures, $T/k_F\tilde{c}\ll 1$, the last two terms can be neglected.

[1] M. Kaveh and N. Wiser, Phys. Rev. B **9**, 4042 (1973).
[2] C. Enz, Helv. Phys. Acta **27**, 199 (1954); Physica **20**, 983 (1954).
[3] J. M. Ziman, *Electrons and Phonons* (Clarendon, Oxford, 1960).
[4] K. L. Ngai and E. J. Johnson, Phys. Rev. Lett. **29**, 1607 (1972); P. J. Lin-Chung and K. L. Ngai, *ibid.* **29**, 1610 (1972); A. K. Ganguly and K. L. Ngai, Phys. Rev. B **8**, 5654 (1973).
[5] R. C. Shukla and E. R. Muller, Phys. Rev. B **21**, 544 (1980).
[6] A. B. Migdal, Zh. Eksp. Teor. Fiz. **34**, 1438 (1958) [Sov. Phys.—JETP **7**, 996 (1958)].
[7] C. Herring, in *Proceedings of the International Conference on Semiconductor Physics, Prague, 1960* (Academic, New York, 1961), p. 60.
[8] N. Wiser, Contemp. Phys. **25**, 211 (1984).
[9] G. D. Mahan, *Many-Particle Physics* (Plenum, New York, 1981).
[10] J. M. Ziman, *Principle of the Theory of Solids* (Cambridge University Press, Cambridge, 1965), p. 207.
[11] C. Kittel, *Introduction to Solid State Physics,* 5th ed. (Wiley, New York, 1976), Table 6.1.
[12] W. A. Harrison, *Electronic Structure and the Properties of Solids* (Freeman, San Francisco, 1980).
[13] A. W. Overhauser, Phys. Rev. Lett. **44**, 489 (1984).
[14] J. Zhao, J. Bass, W. P. Pratt, Jr., and P. A. Schroeder, J. Phys. F **16**, L271 (1986). M. Sinvani, A. J. Greenfield, M. Danino, M. Kaveh, and N. Wiser, J. Phys. F **11**, L73 (1981).